J. Fluid Mech. (1972), *vol.* 56, *part* 3, *pp.* 429–445
Printed in Great Britain

Upwelling of a stratified fluid in a rotating annulus: steady state. Part 1. Linear theory

By J. S. ALLEN

Department of Aerospace Engineering, The Pennsylvania State University

(Received 28 October 1971 and in revised form 24 August 1972)

The linear theory of rotating stratified fluids is applied to describe the steady axisymmetric motion of a stratified fluid in a rotating annulus for values of the stratification parameter $\bar{S} = \sigma N^2/(2\Omega)^2$ that are order one or larger: $\bar{S} \geqslant O(1)$. The motion is mechanically driven by either an applied velocity or by an applied stress at the top surface. The side walls are thermally insulated. Primary attention is given to a study of the meridional, or upwelling circulation. Simple analytical solutions are obtained with the aid of the narrow-gap approximation and a justifiable assumption of an infinite depth. In that case the meridional circulation is confined to a surface Ekman layer and to a Lineykin layer of thickness of $O(\bar{S}^{-\frac{1}{2}})$. It is shown how the solutions for the stress-driven upwelling flow in the annulus apply to a two-dimensional linear model of coastal upwelling in a stratified ocean.

1. Introduction

A linear theory for the effect of a stable density stratification on the steady motion of a contained rotating fluid has been developed by Barcilon & Pedlosky (1967*a*, *b*). Recently, Pedlosky (1970) has worked out, and investigated the stability of, the linear-theory solution for the mechanically driven, axisymmetric flow of a continuously stratified fluid in a rotating annulus, for small values of the stratification parameter $\bar{S} = \sigma N^2/(2\Omega)^2 < O(1)$, where σ is the Prandtl number, N is the Brunt–Väisälä frequency and Ω is the rotational frequency.

In this paper, the linear axisymmetric steady motion of a stratified fluid in a rotating annulus is studied for values of the stratification parameter that are order one or larger: $\bar{S} \geqslant O(1)$. The motion is driven by either an applied velocity or by an applied stress on the top surface. The side walls are thermally insulated. Primary attention is given to a study of the meridional, or upwelling, circulation and the dependence of this circulation on the stratification parameter. The problem of applied stress driving is included for comparison with the applied velocity case and also because the solutions are applicable to a two-dimensional linear model of coastal upwelling in a continuously stratified ocean. The relationship with the oceanic model is discussed in §5.

The narrow-gap approximation is employed and a simplifying, infinite-depth assumption, which does not affect the basic physics, is made. With these approximations, simple analytical solutions are obtained for particular, but illustrative,

forms of the applied velocity or stress. These solutions are presented for a top-surface boundary condition on the perturbation temperature, but the differences in the solutions, when the temperature boundary condition is one of an applied heat flux, are discussed.

This investigation was undertaken to help explain the results of some numerical finite-difference solutions of the steady, axisymmetric, mechanically driven motion of a stratified fluid in a rotating annulus. The purpose of that study, which will be presented in a subsequent paper as part 2 (Allen 1972), was to investigate the nature of the flow when the Rossby number has finite values and to calculate axisymmetric solutions as forerunners of the computation of more complex three-dimensional flows. Many features of the flow, predicted here by the linear theory, have appeared in the finite Rossby number numerical solutions.

2. Formulation

We consider a viscous heat-conducting incompressible fluid, which satisfies the Boussinesq approximation, in a frame of reference rotating with a uniform angular velocity $\Omega = \Omega\hat{\mathbf{k}}$ and acted on by a gravitational acceleration $\mathbf{g} = -g\hat{\mathbf{k}}$ which is antiparallel to the rotation vector. The governing equations for steady motion are

$$\begin{aligned}
\nabla.\mathbf{q} &= 0,\\
\mathbf{q}.\nabla\mathbf{q} + 2\Omega\hat{\mathbf{k}}\times\mathbf{q} &= -(1/\rho_0)\nabla\rho - (\rho/\rho_0)g\hat{\mathbf{k}}\\
&\quad + \tfrac{1}{2}(\rho/\rho_0)\,\Omega^2\nabla|\hat{\mathbf{k}}\times\mathbf{r}|^2 + \nu\nabla^2\mathbf{q},\\
\mathbf{q}.\nabla T &= \kappa\nabla^2 T,\\
\rho &= \rho_0[1-\alpha(T-T_0)],
\end{aligned}$$

where $\mathbf{q}, p, \rho$ and T are respectively the velocity, pressure, density and temperature of the fluid at point $\mathbf{r}$; ν, κ and α are respectively the constant kinematic viscosity, thermometric conductivity and coefficient of thermal expansion; ρ_0 and T_0 are constant reference values of the density and temperature; $\hat{\mathbf{k}}$ is a constant unit vector in the z direction in Cartesian co-ordinates.

We assume that the Froude number $\Omega^2 r_0/g$, where r_0 is a characteristic radial distance from the centre of rotation, is small and consider a linear equilibrium temperature and density distribution (see Greenspan 1968, §1.4) given by

$$T_s = T_0 + \Delta T_0 z/H, \quad \rho_s = \rho_0[1-\alpha\Delta T_0 z/H],$$

where $\Delta T_0 (> 0)$ is the basic temperature difference imposed over the height H.

The variables are non-dimensionalized in the following manner:

$$\begin{aligned}
&\mathbf{q} = U\mathbf{q}^*, \quad \mathbf{r} = H\mathbf{r}^*,\\
&p = p_0 - \rho_0 gHz^* + \tfrac{1}{2}\rho_0 gH\alpha\Delta T_0 z^{*2} + \rho_0 U\Omega H p^*,\\
&T = T_s + (\Omega U/\alpha g)T^*, \quad \rho = \rho_s + (\rho_0 U\Omega/g)\rho^*,
\end{aligned}$$

where p_0 is a constant reference pressure and U is a reference applied velocity. If the motion is driven by an applied stress τ, then we assume $\tau = \tau_0\tau^*$, where τ_0 is a reference value of the applied stress, and we define $U = H\tau_0/\rho_0\nu$ so that the dimensionless interior velocities are of $O(1)$ for $\bar{S} \geqslant O(1)$.

For small Rossby number $\epsilon = U/\Omega L$, such that the nonlinear terms multiplied by ϵ can be neglected, the resulting dimensionless equations are (dropping the asterisks)

$$\nabla . \mathbf{q} = 0, \tag{2.1a}$$

$$2\hat{\mathbf{k}} \times \mathbf{q} = -\nabla p + T\hat{\mathbf{k}} + E\nabla^2 \mathbf{q}, \tag{2.1b}$$

$$4\bar{S}\mathbf{q} . \hat{\mathbf{k}} = E\nabla^2 T, \tag{2.1c}$$

where $E = \nu/\Omega H^2$ is the Ekman number, $\sigma = \nu/\kappa$ is the Prandtl number.

$$N^2 = \alpha g \Delta T_0 / H$$

is the square of the Brunt–Väisälä frequency, $S = N^2/\Omega^2$ and $\bar{S} = \frac{1}{4}\sigma S$. Following Barcilon & Pedlosky (1967*b*) we shall call $\bar{S}$ the stratification parameter. The Ekman number E will be assumed to be small and boundary-layer methods for the limit $E \to 0$ will be used.

The axis of the annulus is aligned with the basic rotation vector. The narrow-gap approximation is used, that is, it is assumed that the distance between the cylindrical side walls is small compared with the mean radius of the annulus. This permits the neglect of the effects of curvature and allows the use of Cartesian co-ordinates (x, y, z) with unit vectors $(\hat{\mathbf{i}}, \hat{\mathbf{j}}, \hat{\mathbf{k}})$. The z co-ordinate direction (vertical direction) is parallel to the axis of the annulus. The x axis is aligned in the radial direction and the y axis is aligned in the azimuthal direction so that, for axisymmetric motion, the flow quantities are independent of y. The side walls of the annulus are vertical and the top and bottom surfaces are horizontal. The origin of the co-ordinates is placed in the plane of the bottom surface so that the fluid is contained in a section $(0 \leqslant x \leqslant 1,\ 0 \leqslant z \leqslant 1)$, where the width has been taken equal to the depth for simplicity.

In Cartesian co-ordinates, with velocity components (u, v, w) in the (x, y, z) directions, and with $\partial/\partial y \equiv 0$, equations (2.1) become

$$u_x + w_z = 0, \tag{2.2a}$$

$$-2v = -p_x + (E\nabla^2 u), \tag{2.2b}$$

$$2u = E\nabla^2 v, \tag{2.2c}$$

$$0 = -p_z + T + (E\nabla^2 w), \tag{2.2d}$$

$$4\bar{S}w = E\nabla^2 T, \tag{2.2e}$$

where the subscripts denote partial differentiation and $\nabla^2 = \partial^2/\partial x^2 + \partial^2/\partial z^2$. The parentheses mark terms that will be neglected in § 3, for the interior flow, and the set of equations with these terms neglected will be referred to as (2·2N).

The boundary conditions are

$$\mathbf{q}(x = 0) = \mathbf{q}(x = 1) = 0, \quad T_x(x = 0) = T_x(x = 1) = 0; \tag{2.3a,b}$$

$$\mathbf{q}(z = 0) = 0, \quad T(z = 0) = 0 \quad [\text{or } T_z(z = 0) = 0]; \tag{2.3c,d}$$

$$\mathbf{q}(z = 1) = V_T(x)\hat{\mathbf{j}}, \tag{2.4a}$$

or

$$\mathbf{q}_z(z = 1) = \tau_T(x)\hat{\mathbf{j}}; \tag{2.4b}$$

$$T(z = 1) = T_T(x), \tag{2.5a}$$

or

$$T_z(z = 1) = T_{Tz}(x); \tag{2.5b}$$

where we assume

$$\int_0^1 T_T \, dx = \int_0^1 T_{Tz} \, dx = 0.$$

3. Analysis

We consider initially the case $\bar{S} = O(1)$. As was shown by Barcilon & Pedlosky (1967*a*), for applied velocity driving, the lowest order interior flow, in an expansion in powers of $E^{\frac{1}{2}}$, is governed by the diffusion equation

$$\nabla^2(\hat{\mathbf{k}}.\nabla \times \mathbf{q} + \tfrac{1}{2}\bar{S}^{-1}T_z) = 0, \tag{3.1}$$

where in general ∇^2 is the full three-dimensional Laplacian operator. A governing equation for the lowest order interior pressure results from (3.1) and is

$$\nabla^2(\bar{S}\nabla_H^2 + \partial^2/\partial z^2)p = 0, \tag{3.2}$$

where ∇_H^2 is the horizontal Laplacian operator. The same equation holds if the driving is by an applied stress. In our case, (3.2) corresponds to the assumption that the interior flow is governed by the balances shown in (2.2) with the terms in parenthesis neglected (equations (2.2N)). Combining (2.2N), we find that

$$\left(\frac{\partial^2}{\partial x^2} + \frac{\partial^2}{\partial z^2}\right)\left(\bar{S}\frac{\partial^2}{\partial x^2} + \frac{\partial^2}{\partial z^2}\right)p = \nabla^2\nabla_L^2 p = 0, \tag{3.3}$$

which corresponds to (3.2) with $\partial/\partial y \equiv 0$. We use the notation

$$\nabla_L^2 = (\bar{S}\partial^2/\partial x^2 + \partial^2/\partial z^2).$$

Barcilon & Pedlosky (1967*a*) also showed that, with applied velocity driving, Ekman layers are absent to the lowest order and the interior $O(1)$ horizontal velocity must itself satisfy the boundary conditions on the top and bottom surfaces. This, along with a boundary condition on the temperature or heat flux, gives two boundary conditions for the pressure at the horizontal surfaces. The boundary conditions on the interior variables at the vertical side walls were also derived. With insulated boundaries a buoyancy layer is not present, to lowest order, and in the axisymmetric case the interior velocity components v and u must satisfy the conditions $v = u = 0$ at the side walls. In terms of the pressure, these conditions are

$$p_x(x = 0, 1) = p_{xxx}(x = 0, 1) = 0. \tag{3.4}$$

The vertical component of velocity, w, derived from the solution to (3.3) will not in general satisfy the side-wall boundary condition (2.3*a*) and will adjust in a thin higher order buoyancy layer that does not affect the lowest order interior flow.

With the boundary condition (3.4) the solution of (3.3) can be written in the form

$$p = \sum_{n=1}^{\infty}\left(\sum_{i=1}^{4} C_{in}e^{\alpha_{in}z}\right)\cos n\pi x, \tag{3.5}$$

where

$$\alpha_{1,2n} = \pm n\pi, \quad \alpha_{3,4n} = \pm \bar{S}^{\frac{1}{2}}n\pi. \tag{3.6a, b}$$

It is clear that the two sets of roots (3.6*a*, *b*) correspond respectively to solutions of the two equations $\nabla^2 p = 0$ and $\nabla_L^2 p = 0$. It is also clear, since

$$|\alpha_{1,2n}|d, \quad |\alpha_{3,4n}|d \geqslant O(1), \tag{3.7}$$

where d stands for the dimensionless depth ($d = 1$ in this case), that the solutions will be primarily determined by the boundary conditions on the top surface and that the homogeneous conditions (2.3c, d) on the bottom surface will only result in relatively small corrections. Consequently, a great deal of simplicity, with no loss of the essential physics, is obtained if we consider the annulus to be of infinite depth. The characteristic length H is assumed to remain unchanged and represents the distance over which the basic temperature difference ΔT_0 is imposed; it naturally loses its significance as the depth of the annulus.

The solution can then be written as the sum of two parts:

$$p = p_I + p_L, \tag{3.8a}$$

where

$$p_I = \sum_{n=1}^{\infty} C_{In} \exp[-n\pi(1-z)] \cos n\pi x, \tag{3.8b}$$

$$p_L = \sum_{n=1}^{\infty} C_{Ln} \exp[-n\pi \bar{S}^{\frac{1}{2}}(1-z)] \cos n\pi x. \tag{3.8c}$$

The solution (3.8) remains valid for $O(1) \leqslant \bar{S} < O(E^{-1})$ and from this point on we consider $\bar{S}$ to be in that range. The second part of the solution is limited, for large values of $\bar{S}$, to a boundary layer on the top surface of thickness of $O(\bar{S}^{-\frac{1}{2}})$. This part of the solution represents a Lineykin layer (Lineykin 1955; Leetma 1971). We point out that, since $\nabla^2 p_I = 0$, it follows that $\nabla^2 v_I = \nabla^2 T_I = 0$ and, consequently, from (2·2N) that $u_I = w_I = 0$. Therefore, a non-zero meridional circulation, u_L and w_L, is associated only with the Lineykin-layer part of the solution. Note also, from (2·2N) and the relations $\nabla^2 p_I = \nabla_L^2 p_L = 0$, that

$$v_{Iz} = \tfrac{1}{2} T_{Ix}, \quad v_{Ix} = -\tfrac{1}{2} T_{Iz}, \tag{3.9a}$$

$$v_{Lz} = \tfrac{1}{2} T_{Lx}, \quad v_{Lx} = -\tfrac{1}{2} \bar{S}^{-1} T_{Lz}, \tag{3.9b}$$

and therefore that the pairs $(v_I, \frac{1}{2}T_I)$ and $(\bar{S}^{\frac{1}{2}} v_L, \frac{1}{2} T_L)$ are conjugate harmonic functions in the variables (x, z) and $(x, \bar{S}^{\frac{1}{2}} z)$, respectively.

3.1. *Applied velocity–applied temperature*

For the case where the boundary condition on the top surface is one of an applied velocity (2.4a) and an applied temperature (2.5a), the boundary values can be expanded in Fourier series of the form

$$V_T(x) = \sum_{n=1}^{\infty} V_{Tn} \sin n\pi x, \quad T_T(x) = \sum_{n=1}^{\infty} T_{Tn} \cos n\pi x. \tag{3.10a,b}$$

Using (3.10) and applying the boundary conditions

$$p_x(z = 1) = 2V_T, \quad p_z(z = 1) = T_T, \tag{3.11a,b}$$

we find that the series solution (3.8) is determined, with

$$C_{In} = -(n\pi)^{-1}(1 - \bar{S}^{-\frac{1}{2}})^{-1}(2V_{Tn} + \bar{S}^{-\frac{1}{2}} T_{Tn}), \tag{3.12a}$$

$$C_{Ln} = (n\pi)^{-1} \bar{S}^{-\frac{1}{2}}(1 - \bar{S}^{-\frac{1}{2}})^{-1}(2V_{Tn} + T_{Tn}). \tag{3.12b}$$

For $\bar{S} = 1$, the two sets of roots (3.6a, b) coincide. The solution is given by the limit, as $\bar{S} \to 1$, of (3.8) and (3.12), or it may be obtained by assuming $\bar{S} = 1$ at the outset and using standard methods for equal roots.

If the top-surface boundary conditions have the particular, but illustrative, form

$$V_T = D_1[D_0 + (1-D_0)x], \quad T_T = 0, \tag{3.13a,b}$$

where D_0 and D_1 are constants ($0 \leqslant D_0 \leqslant 1$, $D_1 = \pm 1$), then the series solutions for $v = v_I + v_L$ and $T = T_I + T_L$, which are obtained from (3.8), can be summed to give the analytical expressions

$$v_I = 2K_0(D_0 v_I^{(0)} + (1-D_0)v_I^{(1)}), \tag{3.14a}$$

$$v_L = -2K_0 \bar{S}^{-\frac{1}{2}}(D_0 v_L^{(0)} + (1-D_0)v_L^{(1)}), \tag{3.14b}$$

where

$$K_0 = D_1 \pi^{-1}(1-\bar{S}^{-\frac{1}{2}})^{-1},$$

$$v_I^{(0)} = \tan^{-1}[\sin \pi x / \sinh \pi(1-z)], \tag{3.15a}$$

$$v_I^{(1)} = \tan^{-1}\left[\frac{\exp[-\pi(1-z)]\sin \pi x}{1+\exp[-\pi(1-z)]\cos \pi x}\right], \tag{3.15b}$$

$$v_L^{(0)} = v_I^{(0)}[x, \bar{S}^{\frac{1}{2}}(1-z)], \quad v_L^{(1)} = v_I^{(1)}[x, \bar{S}^{\frac{1}{2}}(1-z)], \tag{3.15c,d}$$

and

$$T_I = -4K_0[D_0 T_I^{(0)} + \tfrac{1}{2}(1-D_0)T_I^{(1)}], \tag{3.16a}$$

$$T_L = 4K_0[D_0 T_L^{(0)} + \tfrac{1}{2}(1-D_0)T_L^{(1)}], \tag{3.16b}$$

where

$$T_I^{(0)} = \tanh^{-1}[\cos \pi x / \cosh \pi(1-z)], \tag{3.17a}$$

$$T_I^{(1)} = \ln\{1 + 2\exp[-\pi(1-z)]\cos \pi x + \exp[-2\pi(1-z)]\}, \tag{3.17b}$$

$$T_L^{(0)} = T_I^{(0)}[x, \bar{S}^{\frac{1}{2}}(1-z)], \quad T_L^{(1)} = T_I^{(1)}[x, \bar{S}^{\frac{1}{2}}(1-z)]. \tag{3.17c}$$

It is easily shown that a stream function for the meridional flow, such that $u = \psi_z$ and $w = -\psi_x$, is given by the relation

$$\psi = \tfrac{1}{2}E(1-\bar{S}^{-1})v_{Lz}. \tag{3.18}$$

With the boundary conditions (3.13a, b) the solution for ψ, from (3.18) and (3.14b), is

$$\psi = -E(1+\bar{S}^{-\frac{1}{2}})D_1\left\{\frac{D_0 \sin \pi x \cosh \pi \bar{S}^{\frac{1}{2}}(1-z)}{\sinh^2[\pi \bar{S}^{\frac{1}{2}}(1-z)] + \sin^2 \pi x} + \frac{(1-D_0)\exp[-\pi \bar{S}^{\frac{1}{2}}(1-z)]\sin \pi x}{1+2\exp[-\pi \bar{S}^{\frac{1}{2}}(1-z)]\cos \pi x + \exp[-2\pi \bar{S}^{\frac{1}{2}}(1-z)]}\right\}. \tag{3.19}$$

The expression (3.19) is unbounded for $z = 1$, $x \to 0, 1$, which emphasizes the fact that the interior solutions (3.14) and (3.16) are not valid in small regions near the corners. The corner regions will be discussed in more detail in § 4.

The stream function ψ (3.19) gives a solution for the meridional circulation in the Lineykin layer. This circulation must be completed in an Ekman layer on the top surface. Thus, although the Ekman layer certainly does not control the dynamics and, in fact, for these boundary conditions, is essentially driven by the interior and Lineykin-layer solutions, it does play an important role in the meridional circulation.

It is useful, at this point, to think in terms of a perturbation analysis for $\bar{S} > O(1)$ and to consider the solution, away from the corner regions, to be made up of three parts. The first two parts, denoted by subscripts I and L, are already included in our general interior solution and henceforth will be referred to as the

interior and Lineykin-layer solutions, respectively. The third part is the solution for the correction variables in the Ekman layer and will be denoted by a subscript E. The scaling of the lowest order terms with $V_T \neq 0$, as can be checked from (3.12) for the interior and Lineykin-layer variables, is

$$\left.\begin{aligned} T_I &= O(1), & T_L &= O(1), & & \\ v_I &= O(1), & v_L &= O(\bar{S}^{-\frac{1}{2}}), & v_E &= O(E^{\frac{1}{2}}), \\ & & u_L &= O(E\bar{S}^{\frac{1}{2}}), & u_E &= O(E^{\frac{1}{2}}), \\ & & w_L &= O(E), & w_E &= O(E). \end{aligned}\right\} \tag{3.20}$$

The Ekman-layer scaling is determined by the requirement that the vertical velocity w_E should match the vertical velocity w_L of the Lineykin layer at $z = 1$. If the problem were solved by perturbation methods, the terms that would be retained in the Lineykin-layer equations would correspond to (2·2N) with $\nabla^2 \to \partial^2/\partial z^2$. The governing equations for the interior and Lineykin-layer variables would be equivalent to $\nabla^2 p_I = 0$ and $\nabla_L^2 p_L = 0$, respectively, and each would require only one boundary condition at the top surface to determine the solution. The order that would be followed in the application of the boundary conditions at $z = 1$ is

$$\begin{aligned} v_I &= V_T, \quad \text{which determines the interior solution } I; \\ T_I + T_L &= T_T, \qquad\qquad \text{which determines } L; \\ w_L + w_E &= 0. \end{aligned}$$

We note that w_E is determined by the Lineykin-layer solution for w_L. A complete solution for the Ekman layer, however, apparently depends on an analysis of the flow in the corner regions. Note that, as can be checked from (3.19),

$$w_E = -w_L(z = 1)$$

is not related to the Ekman-layer suction velocity that would exist in a homogeneous fluid in a finite-depth annulus with the same applied velocity. This is different from the case with an applied stress driving in § 3.2.

The solutions (3.14), (3.16) and (3.19) are presented, for one set of parameter values, in figure 1 in the form of contour plots of the azimuthal velocity v, the total temperature $\overline{T} = z + (\epsilon/S)T$, and the stream function ψ. The values of the parameters for the case presented are $\bar{S} = 1{\cdot}925$ (corresponding to $\sigma = 7$ and $S = 1{\cdot}1$), $\epsilon = 0{\cdot}1$ and $E = 0{\cdot}0005$, and correspond to a set of parameters used in the numerical experiments in part 2 (Allen 1972). In addition, the finite value of $\epsilon = 0{\cdot}1$ accentuates, and therefore shows clearly, the distortion of the isotherms. The constants in the applied velocity boundary condition (3.13) are $D_0 = 0{\cdot}5$ and $D_1 = -1$ and this corresponds to a motion of the top surface in a sense opposite to the basic rotation. As a result, there is an upwelling of the fluid at the outer side wall ($x = 1$) and a downwelling at the inner wall.

The contours of v and ψ are plotted at equal intervals, between the maximum and minimum values of the variables (listed in the figure caption) in a field which is limited to a depth $d = 1$ (i.e. $0 \leqslant z \leqslant 1$). Note that, with the choice of Rossby number $\epsilon = 0{\cdot}1$, the total temperature has, unrealistically, a maximum value

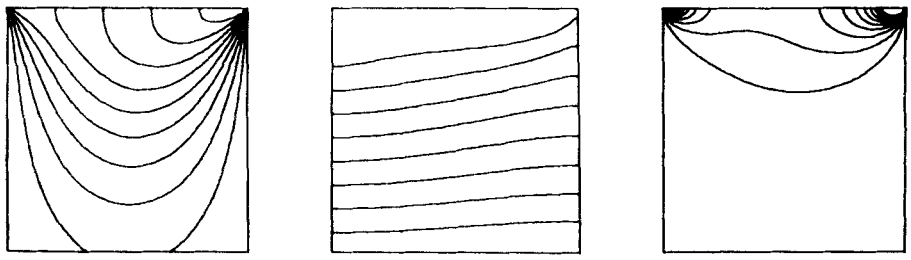

FIGURE 1. Contour plots of the zonal velocity v, the total temperature $\bar{T} = z + (\epsilon/S)T$ and the stream function ψ, for applied velocity driving (3.13) (see §3.1) with $D_0 = 0{\cdot}5$, $D_1 = -1$, $\bar{S} = 1{\cdot}925$, $\epsilon = 0{\cdot}1$ and $E = 0{\cdot}0005$. The maximum and minimum values in the field ($0 \leqslant x \leqslant 1$, $0 \leqslant z \leqslant 1$) and the intervals at which the contours are plotted are $v_{\max} = 0$, $v_{\min} = -1{\cdot}0$, $\Delta v = 0{\cdot}1$; $\bar{T}_{\max} = 1{\cdot}039$, $\bar{T}_{\min} = -0{\cdot}012$, $\Delta\bar{T} = 0{\cdot}105$; $\psi_{\max} = \psi(x = 0{\cdot}9, z = 1) = 27{\cdot}5 \times 10^{-4}$, $\psi_{\min} = 0$, $\Delta\psi = 2{\cdot}75 \times 10^{-4}$. The origin ($x = 0, z = 0$) is at the lower left-hand corner of the plots. v and ψ are plotted at equal intervals between the maximum and minimum values. $\bar{T}$ is plotted at intervals of $\Delta\bar{T} = 0{\cdot}105$ from $\bar{T} = 0{\cdot}105$ to $\bar{T} = 0{\cdot}840$.

greater than one. Because of the singularity of the stream function in the corners, the maximum value of ψ was arbitrarily taken as $\psi_{\max} = \psi(x = 0{\cdot}9, z = 1)$. For the purpose of making the contour plots, the values of the solution were calculated on a uniform rectangular grid with 50 and 64 points in the x and z directions respectively.

The plot of v shows the linear decrease of the applied velocity across the top surface and the nature of the penetration of the surface velocity into the interior. The plot of the isotherms for $\bar{T}$ clearly illustrates the effects of upwelling and downwelling in the corners. The meridional circulation in the Lineykin layer is shown in the plot of the stream function. This circulation is seen to be dominated by intense recirculating eddies in the corners, caused, apparently, by the effect of the non-zero values at $x = 0, 1$ of the applied velocity on the top surface. Even at this moderate value of $\bar{S} = 1{\cdot}925$ most of the transport in the meridional recirculation occurs near the top surface. For increased values of $\bar{S}$ the Lineykin layer decreases in thickness and the circulation crowds closer to the top surface. This circulation pattern should be compared with that which would exist in the original finite depth annulus if the fluid were homogeneous. In that case, the meridional circulation in the interior would involve a downward depth-independent vertical component of flow between Ekman layers on the top and bottom surfaces. There would also be downward flow in boundary layers of thickness $E^{\frac{1}{4}}$ and $E^{\frac{1}{3}}$ on the inner ($x = 0$) side wall. The circulation would be closed by an upwelling of the fluid, from the bottom surface to the top, in vertical $E^{\frac{1}{4}}$ and $E^{\frac{1}{3}}$ layers on the outer side wall.

3.2. *Applied stress–applied temperature*

There are several differences in the solution when the boundary condition is one of an applied stress (2.4b) rather than an applied velocity (2.4a). These can be seen from a consideration of the sequence followed in applying the boundary

conditions. The lowest order scaling for the variables, in a perturbation problem with $\bar{S} > O(1)$ and $\tau_T \not\equiv 0$, is the same as (3.20). The boundary conditions at $z = 1$ are satisfied by the relations

$$v_{Iz} + v_{Lz} + v_{Ez} = \tau_T, \tag{3.21a}$$

$$T_I + T_L = T_T, \quad w_E + w_L = 0. \tag{3.21b,c}$$

Combining (3.21a, b) and using (3.9a, b) we find that the order of application of the boundary conditions is

$$\begin{aligned} v_{Ez} &= \tau_T - \tfrac{1}{2}T_{Tx}, && \text{which determines } E; \\ w_L + w_E &= 0, && \text{which determines } L; \\ T_I + T_L &= T_T, && \text{which determines } I. \end{aligned}$$

The Ekman-layer solution is driven by the quantity $\tau_T - \frac{1}{2}T_{Tx}$, as was pointed out by Leetma (1971). If $T_{Tx} = 0$, the Ekman-layer suction velocity is the same as that which would exist in a homogeneous fluid. The Ekman-layer and Lineykin-layer solutions, and thus the components of the meridional circulation, are determined independently of the interior solution, as was shown in a different manner by Blumsack (1972).

The above results hold for $\bar{S} \geqslant O(1)$ and are needed to determine the solution (3.8). The Ekman-layer suction condition at $z = 1$ is, in this case,

$$w_E = -\tfrac{1}{2}E(\tau_T - \tfrac{1}{2}T_{Tx})_x. \tag{3.22}$$

From (3.18) we obtain

$$w_L = -\tfrac{1}{2}E(1 - \bar{S}^{-1})v_{Lzx}. \tag{3.23}$$

The substitution of (3.22) and (3.23) in (3.21c) yields

$$v_{Lzx}(z = 1) = -(1 - \bar{S}^{-1})^{-1}(\tau_T - \tfrac{1}{2}T_{Tx})_x. \tag{3.24}$$

The surface stress is expanded in a Fourier series of the form

$$\tau_T = \sum_{n=1}^{\infty} \tau_{Tn} \sin n\pi x \tag{3.25}$$

and the surface temperature is given by (3.10b). Conditions (3.24) and (3.21b) are then sufficient to determine the constants in the solution (3.8):

$$C_{In} = -(n\pi)^{-2}(1 - \bar{S}^{-1})^{-1}(2\tau_{Tn} + (n\pi)\bar{S}^{-1}T_{Tn}), \tag{3.26a}$$

$$C_{Ln} = (n\pi)^{-2}\bar{S}^{-\frac{1}{2}}(1 - \bar{S}^{-1})^{-1}(2\tau_{Tn} + (n\pi)T_{Tn}). \tag{3.26b}$$

We note that the series representations (3.10b) and (3.25), when substituted in (3.22), lead to the result

$$\int_0^1 w_E dx = 0. \tag{3.27}$$

Therefore, in the case of a non-vanishing effective stress $\tau_T - \frac{1}{2}T_{Tx}$ at $x = 0, 1$, the derivative of the Fourier series of $\tau_T - \frac{1}{2}T_{Tx}$ in (3.22) must give the correct singular behaviour in the vertical velocity, at $x = 0, 1$, to make the net integrated mass flux (3.27) equal to zero.

If the boundary conditions have the form

$$\tau_T = D_1[D_0 + (1 - D_0)x], \quad T_T = 0, \tag{3.28a,b}$$

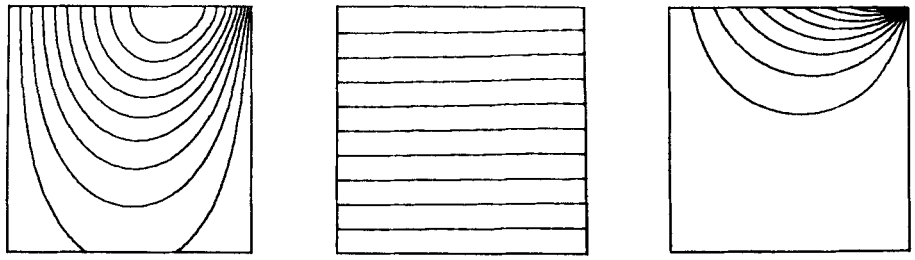

FIGURE 2. Contour plots of v, $\bar{T}$ and ψ for applied stress driving (3·28) (see §3.2) with $D_0 = 0$, $D_1 = -1$, $\bar{S} = 1{\cdot}925$, $\epsilon = 0{\cdot}1$ and $E = 0{\cdot}0005$. The maximum and minimum values and the intervals at which the contours are plotted are $v_{\max} = 0$, $v_{\min} = -0{\cdot}119$, $\Delta v = 0{\cdot}012$; $\bar{T}_{\max} = 1{\cdot}0$, $\bar{T}_{\min} = 0$, $\Delta\bar{T} = 0{\cdot}1$; $\psi_{\max} = 2{\cdot}3 \times 10^{-4}$, $\psi_{\min} = 0$, $\Delta\psi = 0{\cdot}23 \times 10^{-4}$. v, $\bar{T}$ and ψ are plotted at equal intervals between the maximum and minimum values.

then the series solutions for $(v_I + v_L)_z$ and $(T_I + T_L)_z$ can be summed. In terms of (3.15) and (3.17) we obtain

$$v_{Iz} = 2K_1(D_0 v_I^{(0)} + (1 - D_0)v_I^{(1)}), \tag{3.29a}$$

$$v_{Lz} = -2K_1(D_0 v_L^{(0)} + (1 - D_0)v_L^{(1)}), \tag{3.29b}$$

$$T_{Iz} = -4K_1(D_0 T_I^{(0)} + \tfrac{1}{2}(1 - D_0)T_I^{(1)}), \tag{3.30a}$$

$$T_{Lz} = 4K_1\bar{S}^{\frac{1}{2}}(D_0 T_L^{(0)} + \tfrac{1}{2}(1 - D_0)T_L^{(1)}), \tag{3.30b}$$

where $K_1 = D_1\pi^{-1}(1 - \bar{S}^{-1})^{-1}$.

The stream function can be calculated using (3.18):

$$\psi = -D_1\frac{E}{\pi}\left\{D_0\tan^{-1}\left(\frac{\sin\pi x}{\sinh\pi\bar{S}^{\frac{1}{2}}(1-z)}\right) + (1 - D_0)\tan^{-1}\left(\frac{\exp[-\pi\bar{S}^{\frac{1}{2}}(1-z)]\sin\pi x}{1 + \exp[-\pi\bar{S}^{\frac{1}{2}}(1-z)]\cos\pi x}\right)\right\}. \tag{3.31}$$

Contour plots of v, $\bar{T}$ and ψ are presented in figure 2 for the case where $D_0 = 0$ and $D_1 = -1$. The other parameter values are the same as those used in §3.1 for the plots in figure 1. The temperature field T was obtained by numerically integrating (3.30a, b), with the same grid spacing as that used in §3.1, from $z = 1$ to $z = 0$, using the boundary condition (3.21b) at $z = 1$. The velocity field was obtained by using (3.9a, b) and numerically integrating (3.30a, b) from $x = 0$ to $x = 1$, using the boundary condition $v(x = 0) = 0$. The condition $v(x = 1) \simeq 0$ was recovered at $x = 1$. The values of the stream function (3.31) are finite and the maximum value occurs in the corner $z = 1$, $x \to 1$. For the plot, however, we used $\psi_{\max} = \psi(x = 0{\cdot}94, z = 1)$.

The Lineykin-layer circulation, in this case, is characterized by concentrated upwelling in the corner $(x = 1, z = 1)$ where the applied stress has a non-zero negative value. The fluid then flows from the corner out towards $x = 0$ in the surface Ekman layer, where it is returned at a uniform rate, corresponding to the linear variation of surface stress, to the Lineykin layer. The nature of this

circulation, which has no side-wall boundary-layer character at all, is clearly shown in the plot of ψ.

The zonal velocity v has a maximum absolute value on the top surface, $z = 1$, at a value of x that apparently depends on the particular stress distribution. For the case of a uniform stress, $D_0 = +1$, $D_1 = -1$, the solution is symmetric about $x = 0{\cdot}5$ and the maximum absolute value of v naturally occurs at $x = 0{\cdot}5$. For the case in figure 2, the position of the maximum absolute value, which is found by using (3.9*a*, *b*) and identifying the point where $v_x(z = 1) = 0$, is $x = \frac{2}{3}$. The distortion of the isotherms of the total temperature T_T is relatively slight. For these parameter settings the upwelling circulation in the stress-driven case is weaker than in the velocity-driven case of figure 1.

3.3. *Applied velocity–applied heat flux*

In the case where the boundary conditions for an applied velocity (2.4*a*) and an applied heat flux (2.5*b*) are used, the scaling, for a perturbation solution, is

$$\left.\begin{aligned} T_I = O(1), \quad & T_L = O(\bar{S}^{-\frac{1}{2}}), & \\ v_I = O(1), \quad & v_L = O(\bar{S}^{-1}), & v_E = O(E^{\frac{1}{2}}\bar{S}^{-\frac{1}{2}}), \\ & u_L = O(E), & u_E = O(E^{\frac{1}{2}}\bar{S}^{-\frac{1}{2}}), \\ & w_L = O(E\bar{S}^{-\frac{1}{2}}), & w_E = O(E\bar{S}^{-\frac{1}{2}}). \end{aligned}\right\} \tag{3.32}$$

The solution is determined by the application of the boundary conditions in the sequence

$$\begin{aligned} v_I &= v_T, \quad \text{which determines } I; \\ T_{Iz} + T_{Lz} &= T_{Tz}, \quad \text{which determines } L; \\ w_L + w_E &= 0. \end{aligned}$$

Compared with the applied velocity–applied temperature case of §3.1, the Ekman- and Lineykin-layer solutions are weaker in magnitude by $O(\bar{S}^{-\frac{1}{2}})$.

3.4. *Applied stress–applied heat flux*

For applied stress (2.4*b*) and applied heat flux (2.5*b*) boundary conditions, the scaling, in a perturbation analysis, is the same as (3.32). The order in which the boundary conditions are applied is

$$v_{Iz} = \tau_T, \quad \text{which determines } I; \tag{3.33a}$$

$$T_{Iz} + T_{Lz} = T_{Tz}, \quad \text{which determines } L; \tag{3.33b}$$

$$w_L + w_E = 0. \tag{3.33c}$$

The surface stress is balanced directly by the interior velocity, in contrast to the applied stress–applied temperature case of §3.2, where it is balanced by the Ekman-layer component. Compared with the solution in §3.2, the Ekman- and Lineykin-layer components are smaller in magnitude by $O(\bar{S}^{-\frac{1}{2}})$.

In this problem, and that in §3.3, the general series solution (3.8) is easily determined by applying the appropriate boundary conditions (2.4) and (2.5). Analytical solutions are again obtainable for velocity and stress driving functions

of the form (3.13a) and (3.28a). For this case, it can be shown from the series solution (3.8) that, if $T_{Tz} = 0$,

$$w_L(z = 1) = \tfrac{1}{2}E(1+\bar{S}^{-\frac{1}{2}})\bar{S}^{-\frac{1}{2}}\tau_{Tx}.$$

Thus, although the surface stress is balanced by the interior velocity, the Ekman-layer normal velocity is still related, albeit in an indirect manner and with a different proportionality constant than in § 3.2, to the curl of the applied stress.

4. Corner region

The solutions obtained in § 3 are not valid in small regions in the corners $z \to 1$, $x \to 0, 1$. In fact, the interior and Lineykin-layer solutions may be singular at the corner points as was mentioned in connexion with (3.19). For $\bar{S} < O(1)$, the corner regions have the familiar scaling $\delta_x = \delta_z = O(E^{\frac{1}{2}})$ and, to lowest order, the effects of stratification are not important. For $\bar{S} = O(1)$, the x and z scaling remain the same, but the effects of stratification are important. In this case, all the terms in (2.2) have to be retained. For $\bar{S} > O(1)$, however, a scale analysis shows that an $E^{\frac{1}{2}} \times E^{\frac{1}{2}}$ corner region is not present and that it is replaced by two regions with scaling

(i) $$\delta_x = O(E^{\frac{1}{2}}\bar{S}^{\frac{1}{2}}), \quad \delta_z = O(E^{\frac{1}{2}}), \tag{4.1a}$$

and

(ii) $$\delta_x = \delta_z = O(E^{\frac{1}{2}}\bar{S}^{-\frac{1}{4}}). \tag{4.1b}$$

Only the case $\bar{S} > O(1)$ will be considered here. In corner region (i), the terms in (2.2) that enter in the lowest order balance are

$$u_x + w_z = 0, \tag{4.2a}$$

$$-2v = -p_x + Eu_{zz}, \quad 2u = Ev_{zz}, \tag{4.2b, c}$$

$$0 = -p_z + T, \quad 4\bar{S}w = ET_{zz}. \tag{4.2d, e}$$

Equations (4.2) are essentially just a combination of the Ekman- and Lineykin-layer equations and the terminology Ekman–Lineykin corner region will be used.

Corner region (ii) has the same scaling (4.1b) as the buoyancy layer (Barcilon & Pedlosky 1967b) and will be called the buoyancy corner region. In the lowest order balance in this region, all the terms in (2.2a, c, d, e) enter and (2.2b) becomes $0 = -p_x + E\nabla^2 u$.

We shall examine the solution in the corner at $x = 1, z = 1$ only for the applied stress–applied temperature case of § 3.2. Because of the singular behaviour of the Lineykin-layer solution at the corners, it is advantageous to abandon the use of correction variables and to consider the Ekman- and Lineykin-layer parts of the solution to be represented by a separate expansion which is valid in a region around $x = 1, z = 1$.

For the Ekman–Lineykin corner region (4.1a), the variables are stretched and expanded in the following manner:

$$\xi = (1-x)E^{-\frac{1}{2}}\bar{S}^{-\frac{1}{2}}, \quad \zeta = (1-z)E^{-\frac{1}{2}};$$

$$u = E^{\frac{1}{2}}u_0(\xi, \zeta) + \ldots, \quad v = E^{\frac{1}{2}}v_0 + \ldots, \quad w = E^{\frac{1}{2}}\bar{S}^{-\frac{1}{2}}w_0 + \ldots,$$

$$T = E^{\frac{1}{2}}\bar{S}^{\frac{1}{2}}T_0 + \ldots, \quad p = E\bar{S}^{\frac{1}{2}}p_0 + \ldots.$$

It is advantageous to introduce a stream function ψ_0 (Blumsack 1972) such that $u_0 = -\psi_{0\zeta}$, $w_0 = \psi_{0\xi}$, i.e. $\psi = E\psi_0(\xi, \zeta) + \ldots$. One equation for ψ_0 can be derived from the scaled form of (4.2) and is

$$\frac{\partial^6 \psi_0}{\partial \zeta^6} + 4\frac{\partial^2 \psi_0}{\partial \xi^2} + 4\frac{\partial^2 \psi_0}{\partial \zeta^2} = 0. \tag{4.3}$$

The boundary conditions for (4.3), at $\zeta = 0$, come from the relations

$$\psi(z = 1) = 0, \quad u_z = \psi_{zz}(z = 1) = 0, \tag{4.4a, b}$$

$$\psi_{zzzz}(z = 1) = -E^{-1}2(v_z - \tfrac{1}{2}T_x) = -E^{-1}2(\tau_T - \tfrac{1}{2}T_{Tx}). \tag{4.4c}$$

Condition (4.4*c*) will force a ψ of magnitude $\psi = O(\delta_z^4 E^{-1}) = O(E)$, which is consistent with our scaling and with the magnitude of the interior value (3.31). The resulting boundary conditions for ψ_0 are

$$\psi_0(\zeta = 0) = \psi_{0\zeta\zeta}(\zeta = 0) = 0, \tag{4.5a, b}$$

$$\psi_{0\zeta\zeta\zeta\zeta}(\zeta = 0) = -2[\tau_T(x = 1) - \tfrac{1}{2}T_{Tx}(x = 1)], \tag{4.5c}$$

$$\psi_0(\xi = 0) = 0. \tag{4.5d}$$

In addition, we require that $\psi_0(\xi \to \infty)$ be bounded and that $\psi_0(\zeta \to \infty) \to 0$.

For the buoyancy corner region (4.1*b*), an equation for the stream function, which is also of sixth order in z, can be derived and boundary conditions from (4.4) are again applicable. However, in this case (4.4*c*) only requires $\psi = O(E\bar{S}^{-1})$, which is smaller than $O(E)$. The boundary conditions at $x = 1$ will be homogeneous and, evidently, an $O(E)$ stream function will not exist in the buoyancy corner region since it is not required by the boundary conditions at the surfaces or by the matching with $\psi_0(\xi, \zeta)$. Consequently, in this problem the buoyancy corner region is not involved in the determination of the lowest order stream function.

We note that an unscaled form of (4.3) could be easily solved, with the appropriate boundary conditions, for $0 \leqslant x \leqslant 1$ with the use of a Fourier sine series in x. The solution should give a uniformly valid approximation for the total meridional circulation.

The solution to (4.3), with boundary conditions (4.5) and with $T_T = 0$, can be obtained with the aid of a Fourier sine transform in ζ and is

$$\psi_0 = \int_0^\infty \hat{\psi}_0(\xi, \lambda) \sin \lambda\zeta \, d\lambda, \tag{4.6}$$

where

$$\hat{\psi}_0(\xi, \lambda) = -\frac{4\tau_T(x = 1)}{\pi\lambda(\lambda^4 + 4)}[1 - \exp(-\tfrac{1}{2}\lambda(\lambda^4 + 4)^{\frac{1}{4}}\xi)]. \tag{4.7}$$

For $\zeta \gg 1$, (4.6) can be evaluated approximately by contour integration and the use of Laplace's method along the imaginary λ axis. The result is

$$\psi_0 \approx -\tau_T(x = 1)\pi^{-1} \tan^{-1}(\xi/\zeta). \tag{4.8}$$

For $\xi \gg 1$ and $\zeta = O(1)$, contour integration can be used for the first part of (4.7) and Laplace's method can be applied directly to the second part to give

$$\psi_0 \approx -\tau_T(x = 1)[-\tfrac{1}{2}e^{-\zeta}\cos\zeta + \pi^{-1}\tan^{-1}(\xi/\zeta)]. \tag{4.9}$$

The expressions (4.8) and (4.9) match with the Ekman-layer solution and with the stream-function solution (3.31), when it is expanded for $(1-x) \ll 1$, $\bar{S}^{\frac{1}{2}}(1-z) \ll 1$. The behaviour (4.8), where the streamlines lie along the straight lines $\xi/\zeta =$ constant, can be seen in figure 2 and is the same as that derived by Blumsack (1972), for $\bar{S} \leqslant O(1)$, in a region that corresponds, in our case, to $O(E^{\frac{1}{2}}\bar{S}^{-\frac{1}{2}}) \ll 1-z \ll O(\bar{S}^{-\frac{1}{2}})$, $1-x \ll 1$. Note that this local behaviour is independent of the distribution of the stress and depends only on the fact that

$$\tau_T(x=1) \neq 0.$$

For the applied velocity–applied temperature boundary condition (3.13) in § 3.1, the stream function (3.19) at $z = 1$ is

$$\psi(z=1) = -E(1+\bar{S}^{-\frac{1}{2}})D_1[D_0(\sin\pi x)^{-1} + (1-D_0)\tfrac{1}{2}\sin\pi x(1+\cos\pi x)^{-1}], \quad (4.10)$$

which is unbounded at $x = 0, 1$. Expanding (4.10) for $1-x \ll 1$ and substituting $1-x = O(E^{\frac{1}{2}}\bar{S}^{\frac{1}{2}})$, we surmise that the magnitude of the maximum value of ψ will have a dependence on the parameters of the form $\psi = O[E^{\frac{1}{2}}\bar{S}^{-\frac{1}{2}}(1+\bar{S}^{-\frac{1}{2}})]$. This is greater than the estimate $\psi = O[E(1+\bar{S}^{-\frac{1}{2}})]$ obtained for $0 < x < 1$, and reflects the strength of the recirculating eddies near the corners.

An important point to note about the Ekman–Lineykin corner region is that horizontal diffusion terms are not included in the primary balances. This is in contrast to the $E^{\frac{1}{2}} \times E^{\frac{1}{2}}$ corner region, for $\bar{S} \leqslant O(1)$, where horizontal friction terms are definitely important. Apparently, for strong stratification $\bar{S} > O(1)$ the presence, in the surface Ekman layer, of a vertical boundary is felt through the effects of horizontal temperature and pressure gradients. As a result, for $\bar{S} > O(1)$, horizontal diffusion plays no direct role in the lowest order upwelling circulation with applied stress–applied temperature driving. Horizontal diffusion remains important, of course, in the balances involving the interior flow component.

5. Coastal upwelling models

Linear two-dimensional steady-state models of coastal upwelling in a continuously stratified ocean with uniform rotation have been considered by Leetma (1969; see also 1971), Hsueh & Kenney (1972) and Blumsack (1972). The results of the analysis of the stress-driven annulus flow in § 3.2 apply to these upwelling models and provide useful explicit solutions in a parameter range not previously considered. The relationship between the annulus flow and the oceanic models is discussed below.

If constant eddy coefficients are used to represent turbulent exchange processes, then linear equations which are similar to (2.2) arise in two-dimensional models of coastal upwelling (with the two dimensions being in a plane normal to the coast) in which the β-effect is neglected. The main difference in the problem formulation comes from the fact that the oceanic motions have characteristic vertical scales H which are much smaller than the characteristic horizontal scales L and also have vertical eddy coefficients, for momentum A_V and for apparent temperature K_V, which differ in magnitude from the horizontal eddy coefficients A_H and K_H.

In forming dimensionless equations for the ocean models, therefore, the procedure is similar to that used in arriving at (2.2) with the exception that the horizontal co-ordinates (x, y) and velocity components (u, v) are non-dimensionalized with L and U, respectively, whereas z and w are non-dimensionalized with H and UH/L. The resulting linear dimensionless equations are

$$u_x + w_z = 0, \tag{5.1a}$$

$$-2v = -p_x + E_H u_{xx} + E_V u_{zz}, \tag{5.1b}$$

$$2u = E_H v_{xx} + E_V v_{zz}, \tag{5.1c}$$

$$0 = -p_z + T + \delta^2 E_H w_{xx} + \delta^2 E_V w_{zz}, \tag{5.1d}$$

$$4\bar{S}\delta^2 w = (E_H/\sigma_H) T_{xx} + (E_V/\sigma_V) T_{zz}, \tag{5.1e}$$

where $\delta = H/L$, $E_H = A_H/\Omega L^2$, $E_V = A_V/\Omega H^2$, $\sigma_H = A_H/K_H$ and $\sigma_V = A_V/K_V$. Since $\delta \ll 1$, (5.1*d*) results, for almost all flow regions, in a hydrostatic balance.

The similarity with the annulus case depends on the assumption that $\sigma_V = \sigma_H$ and is most easily seen if the characteristic vertical scale H is chosen so that $E_V = E_H$, i.e. $H = L(A_V/A_H)^{\frac{1}{2}}$. Equations (5.1) then reduce to the same form as (2.2) with $4\bar{S}\delta^2$ replacing $4\bar{S}$ in (2.2*e*) and $\delta^2 E_H$ replacing E in (2.2*d*). This is essentially the set of equations that was used in the previously mentioned papers to study the steady motion, induced by an applied stress and temperature, near a single thermally insulated, vertical coast. Leetma (1969) neglected the effects of horizontal diffusion entirely in a finite-depth model where the depth d was in the range $E_V^{\frac{1}{2}} < d < \delta\bar{S}^{\frac{1}{2}}$. Hsueh & Kenney (1972) examined the steady response of a stratified fluid of infinite depth to a single Fourier component of the applied stress which vanishes at the coast. Blumsack (1972) considered an infinite-depth model for $\delta^2\bar{S} \leqslant O(1)$, with a non-vanishing stress at the coast, and obtained a solution for the stream function in terms of Fourier transforms. Approximate, locally valid, analytical expressions were given for three regions of the flow near the upwelling corner.

Since, for the annulus flow with $\bar{S} \geqslant O(1)$, the term $\nabla^2 w$ in (2.2*d*) does not enter in the determination of the interior or Lineykin-layer solutions, the dimensionless equations that are solved are the same as those used in the oceanic models. The annulus solutions, therefore, transform directly to solutions of the oceanic model, with $\delta^2\bar{S} \geqslant O(1)$, if the following substitutions are made: $E \to E_H = E_V$, $\bar{S} \to \delta^2\bar{S} = (A_V/A_H)\bar{S}$, $H \to L$ (for the non-dimensionalization of the horizontal co-ordinate), $H \to L(A_V/A_H)^{\frac{1}{2}}$ and $U \to U(A_V/A_H)^{\frac{1}{2}}$ (for the non-dimensionalization of the vertical co-ordinate and the vertical velocity). The series solution (3.8) can be used for finite- or infinite-depth cases in which a fluid of semi-infinite horizontal extent is adjacent to a single coast if the driving is assumed to be periodic. Although the analytical solutions (3.29)–(3.31) correspond, when extended periodically, to discontinuous stress distributions, they are useful in giving an explicit example of how the corner behaviour (4.8), caused by a non-vanishing stress at the coast, is linked to the Lineykin- and Ekman-layer solutions.

An attractive feature of the annulus solutions, concerning their possible oceanic relevance, is provided by the predicted nature of the upwelling circulation, as shown in figure 2. The upwelling fluid enters the surface layer in the corner near the vertical boundary. The inflow to the upwelling corner comes, however, through the Lineykin layer from regions away from the boundary. There is no involvement of the flow in a side-wall boundary layer. As a result, the predicted upwelling circulation looks very reasonable compared with what one might expect in a coastal upwelling zone, over a continental shelf, in the ocean. This circulation should be contrasted with that which would exist in a finite-depth two-dimensional model with a homogeneous fluid. In that case the upwelling fluid would come directly from an Ekman layer on the bottom in side-wall boundary layers of thickness $E^{\frac{1}{4}}$ and (for $\delta \ll E^{\frac{1}{2}}$)$E^{\frac{1}{2}}$.

For an oceanic model with dimensional depth D, the condition (3.7), for the applicability of the infinite-depth approximation, reduces to

$$\min\left[\pi(D/L)\,(A_H/A_V)^{\frac{1}{2}},\ \pi(D/L)\bar{S}^{\frac{1}{2}}\right] \geqslant O(1), \tag{5.2}$$

where L is the largest relevant horizontal scale (half wavelength) of the applied driving. The appropriateness, for the oceanic case, of (5.2) and of the condition

$$\delta^2\bar{S} = (A_V/A_H)\bar{S} \geqslant O(1) \tag{5.3}$$

is hard to estimate because of large uncertainties in the values of A_V, A_H and L. However, let us consider a particular upwelling region, for example that on the continental shelf off the coast of Oregon (see e.g. Collins *et al.* 1968), and try to make some estimates. Assuming that $D = 200\,\mathrm{m} = 2\times10^4\,\mathrm{cm}$, $N^2 = 10^{-4}\,\mathrm{s}^{-2}$ (corresponding to a change in density $\Delta\rho/\rho \simeq 2\times10^{-3}$, over the distance D), $2\Omega = 10^{-4}\,\mathrm{s}^{-1}$ and $\sigma = 1$, we obtain $\bar{S} = 10^4$. If we assume that the eddy coefficients are in the ranges $A_H = 10^6$–$10^8\,\mathrm{cm}^2/\mathrm{s}$ and $A_V = 10$–$10^2\,\mathrm{cm}^2/\mathrm{s}$ and that $L = 50\,\mathrm{km} = 5\times10^6\,\mathrm{cm}$, then we find that

$$\begin{aligned}
\pi(D/L)\,(A_H/A_V)^{\frac{1}{2}} &\approx 39{\cdot}7 - 1{\cdot}26,\\
\pi(D/L)\bar{S}^{\frac{1}{2}} &\approx 1{\cdot}26,\\
(A_V/A_H)\bar{S} &\approx 1\text{–}10^{-3}.
\end{aligned}$$

We see that an assessment of the validity of the conditions (5.2) and (5.3) depends critically on the values chosen for A_V, A_H and L. The above numbers, if they are representative, show that the approximations are questionable for this case.

It should be mentioned that the use of two-dimensional models, with uniform rotation, to study coastal upwelling is open to question. In that connexion, the results, which concern upwelling, from linear theories of the circulation in a homogeneous ocean (Pedlosky 1968; Durance & Johnson 1970) might offer some guidance. In those models the β-effect is important because, although it does not affect the upwelling dynamics directly, it influences the nature of the interior flow so that the fluid required to balance the offshore transport in the surface Ekman layer is fed to the upwelling boundary layer uniformly over the depth. With uniform rotation the fluid can come directly from the bottom in a side-wall boundary layer. Another result from the homogeneous β-plane models is that

the interior inflow of fluid, to the upwelling boundary layer, is geostrophically balanced by pressure gradients in the longshore direction (see also Garvine 1971). This possibility is, of course, excluded in the two-dimensional models. The importance of these effects in more realistic flows, which include stratification, nonlinearities, realistic coastal bottom topography, etc., has not been determined.

The author wishes to thank Dr J. J. O'Brien for interesting him in the phenomenon of coastal upwelling. The contour plots were made with the computer facilities of the National Center for Atmospheric Research, which is sponsored by the National Science Foundation. This research was partially supported by the Atmospheric Science Section, National Science Foundation, under NSF Grant GA-18109 and by the Oceanography Section, National Science Foundation, under NSF Grant GA-30592.

REFERENCES

ALLEN, J. S. 1972 Upwelling of a stratified fluid in a rotating annulus. Part 2. Numerical solutions. Submitted to *J. Fluid Mech.*

BARCILON, V. & PEDLOSKY, J. 1967*a* Linear theory of rotating stratified fluid motions. *J. Fluid Mech.* **29**, 1–16.

BARCILON, V. & PEDLOSKY, J. 1967*b* A unified linear theory of homogeneous and stratified rotating fluids. *J. Fluid Mech.* **29**, 609–621.

BLUMSACK, S. L. 1972 The transverse circulation near a coast. *J. Phys. Oceanogr.* **2**, 34–40.

COLLINS, C. A., MOOERS, C. N. K., STEVENSON, M. R., SMITH, R. L. & PATTULLO, J. G. 1968 Direct current measurements in the frontal zone of a coastal upwelling region. *J. Oceanogr. Soc. Japan*, **24**, 295–306.

DURANCE, J. A. & JOHNSON, J. A. 1970 East coast ocean currents. *J. Fluid Mech.* **44**, 161–172.

GARVINE, R. W. 1971 A simple model of coastal upwelling dynamics. *J. Phys. Oceanogr.* **1**, 169–179.

GREENSPAN, H. P. 1968 *The Theory of Rotating Fluids.* Cambridge University Press.

HSUEH, Y. & KENNEY, R. N. 1972 Steady coastal upwelling in a continuously stratified ocean. *J. Phys. Oceanogr.* **2**, 27–33.

LEETMA, A. 1969 On the theory of coastal upwelling. Ph.D. thesis, M.I.T.

LEETMA, A. 1971 Some effects of stratification on rotating fluids. *J. Atmos. Sci.* **28**, 65–71.

LINEYKIN, P. S. 1955 On the determination of the thickness of the baroclinic layer in the ocean. *Dokl. Akad. Nauk SSSR*, **101**, 461–464.

PEDLOSKY, J. 1968 An overlooked aspect of the wind-driven oceanic circulation. *J. Fluid Mech.* **32**, 809–821.

PEDLOSKY, J. 1970 *Notes on the* 1970 *Summer Program in Geophysical Fluid Dynamics, The Woods Hole Oceanographic Institution*, no. 70–50, vol. **1**, 1–67.